Characterizing Radiation-Induced Oxidation of DNA by Way of the Monohydrated Guanine-Cytosine Radical Cation

ARTICLE *in* THE JOURNAL OF PHYSICAL CHEMISTRY B · MAY 2009

Impact Factor: 3.3 · DOI: 10.1021/jp900444k

Characterizing Radiation-Induced Oxidation of DNA by Way of the Monohydrated Guanine−Cytosine Radical Cation

Heather M. Jaeger* and Henry F. Schaefer III

Center for Computational Quantum Chemistry, University of Georgia, Athens, Georgia 30602-2556

Received: January 15, 2009; Revised Manuscript Received: April 7, 2009

The interaction of one water molecule with the guanine−cytosine radical cation has been studied with *ab initio* and density functional methods in order to help elucidate the nature of oxidized aqueous DNA. The theoretical spin density of $[GC]^{\bullet+}$ reveals that the radical center is localized on guanine. The adiabatic ionization potential lowers from 7.63 to 6.71 eV in concurrence with the formation of the Watson−Crick base pair and hydration by one water molecule. A natural bond orbital analysis of partial charges shows that approximately 80% of the positive charge persists on guanine upon hydration and formation of the Watson−Crick base pair with cytosine. Hydration energies were computed with second-order Z-averaged perturbation theory (ZAPT2) using the aug-cc-pVDZ basis set at 11 stationary points on the B3LYP/DZP++ potential energy surface. The hydration energy at the global minimum is 14.2 kcal mol^{-1}. The lowest energy structures correspond to hydration near the glycosidic bond sites. Structural changes in the Watson−Crick base pair are predominantly seen for monohydration in the groove regions of double-helix DNA.

Introduction

The complex and intertwining physical, chemical, and biological processes leading to physiological alterations from irradiated living cells can best be approached from the underlying physical properties of the molecules at work. In this regard, much attention has been focused on primary direct radiation products in aqueous DNA.[1−13] These products, consisting of various radical cations, are detected through electron spin resonance (ESR) or electron−nuclear double resonance (ENDOR) spectra. However, the energetic barriers that distinguish initial (primary) kinetic products and thermal products are readily overcome at ambient temperatures, and subsequent distonic deprotonation states are often difficult to detect.[14] Quantum mechanical studies on radiation products do not suffer from ambiguity but are inhibited by the size or scope of the radiation target.

A radiation target may contain multiple oxidation sites at which a single electron is removed. However, the product resulting from oxidation of the target, regardless of "where" the electron loss occurred, is the same. If the initial ionization event occurs on the DNA backbone, on a nearby water molecule, or on one of the other DNA bases, the damage is transferred to a guanine base. This phenomenon can be attributed to barrierless or low-barrier electron hole migration. Proposed pathways[15−17] for hole transfer in irradiated aqueous DNA (Figure 1) comprise a complicated scenario in which the primary radical site resides on guanine.[7,13,18−22] Sugar radicals have also been observed from irradiated DNA and, following Bragg's Law, comprise 30−40% of the total radical species.[23,24]

The ability for guanine to act as an effective radical trap is related to its ionization potential. Guanine has the lowest ionization potential of all individual DNA constituents in the gas phase,[25−32] and hydrogen-bonding interactions with surrounding molecules lower the IP of guanine further.[33−36] Hydrogen-bonds formed from hydrating water molecules and

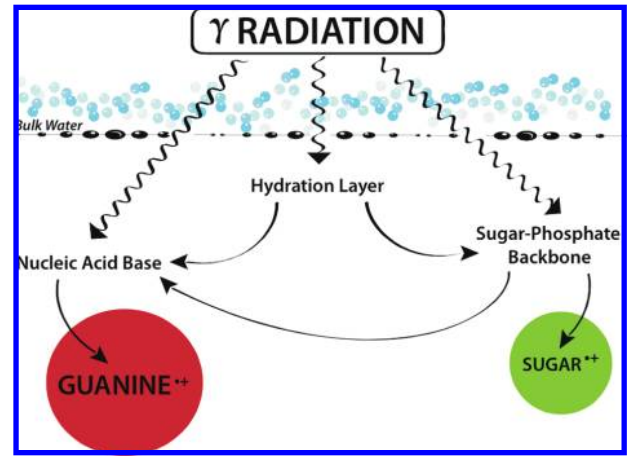

Figure 1. Electron hole migration pathways in irradiated aqueous DNA. The size of the guanine and sugar radical cation circles is approximately proportionate to the observed formation efficiency for each species.

base pairing uniformly lower the IP of DNA bases, facilitating long-range charge transfer through the DNA "π-way". Neighboring, noncovalently bound molecules are intimately tied to molecular targets such that the outcome of ionization events depends heavily on their presence.[37] Incorporating cytosine and a single water molecule with guanine creates a suitable model for primary direct radiation products resulting from γ-ray and X-ray irradiation of DNA.

Increasing the collective radiation target to include neighboring, noncovalently bound molecules introduces the possibility for many different cluster structures of the oxidized species. Theoretical studies have focused on the increased stability of stacked nucleic acid base dimers relative to planar Watson−Crick dimers in solution.[38−41] Only neutral species have been investigated so far. The change in the relative energies of stacked and Watson−Crick base pairs are driven by the system's natural tendency to maximize the total interaction energy. Water

* To whom correspondence should be addressed. E-mail: jaeger@ccqc.uga.edu.

10.1021/jp900444k CCC: $40.75
Published on Web 05/15/2009

interacts more strongly around the perimeter of nucleic acid bases than above or below the base pair plane.[42−52] The strong interaction of base pairs in Watson−Crick or Hoogsteen arrangements is eventually overcome by hydration energy.

The positive charge on $[GC]^{\bullet+}$ creates charge−dipole interactions between water and the base pair that are not present in the neutral species.[53] This effect alters the interaction such that the behavior of the solvated cation does not resemble that of the neutral. However, one should expect that the global minimum structure of the monohydrated cation dimer exists as a Watson−Crick pair, as is the case for the neutral species.[54] And, that the hydration energies and hydration structure of the first shell are distinctly different from the neutral guanine−cytosine dimer results.

The interaction energies and charge distribution at all minima on the Watson−Crick $[GC\cdots H_2O]^{\bullet+}$ potential energy surface indicate which hydration sites are the most important for hole migration pathways leading to the guanine radical. The equilibrium structures of $[GC\cdots H_2O]^{\bullet+}$ also contain information concerning the hydration effects on DNA conformations. Specifically, changes are tracked in Watson−Crick hydrogen bond distances, indicating which hydration sites are responsible for inducing structural changes in double helix DNA.

Theoretical Methods

All stationary point structures, including transition states, were obtained using unrestricted Kohn−Sham density function theory (DFT) with the B3LYP functional implemented in Q-Chem 3.1.[55] A double-ζ quality basis set with polarization and diffuse functions (DZP++)[56−58] was employed for all density functional calculations. Subsequently, harmonic vibrational frequencies were computed via analytic second derivatives at each stationary point with the same level of theory. The integration quadrature consisted of 75 radial shells and 302 angular points per shell. In addition to the monohydrated GC radical cation, geometry optimizations were carried out on $G^{\bullet+}$, C, H_2O, and the guanine−cytosine radical cation dimer.

The $G^{\bullet+}$−C interaction energy in the Watson−Crick arrangement was evaluated using the supramolecule approach.

$$\Delta E_{WC} = E_{GC+} - E_{G+} - E_C \quad (1)$$

E_{GC+} is the energy of the Watson−Crick guanine−cytosine cation dimer. E_{G+} and E_C are the energies of the isolated monomers. The hydration energy, ΔE_{HYD}, was predicated in a similar manner for every equilibrium structure of the monohydrated $[GC]^{\bullet+}$.

$$\Delta E_{HYD} = E_{GCW+} - E_{GC+} - E_W \quad (2)$$

E_{HYD} encompasses the relative energies of the trimer minima and transition states considering that differences between the hydration energies and respective total energies are constant. The global minimum of $[GC\cdots H_2O]^{\bullet+}$ is the structure with the largest hydration energy.

Hydration energies were computed using the B3LYP/DZP++ and *Z*-averaged second-order perturbation theory (ZAPT2)/aug-cc-pVDZ levels of theory. Dunning's correlation-consistent aug-cc-pVDZ[59,60] basis set was chosen for its modest size and inclusion of diffuse functions. Multiple sets of *d* polarization functions on the heavy atoms are important for hydrogen-bonding energies, whereas higher angular momentum functions have been shown to contribute less.[61] The counterpoise correction was not applied to the evaluation of hydration energies, as it does not improve the accuracy of MP2 interaction energies for hydrogen-bonded systems with medium-sized basis sets.[62]

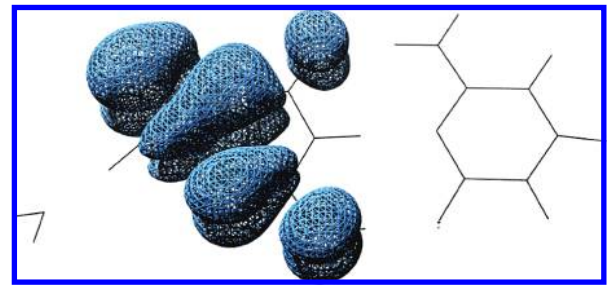

Figure 2. $[GC\cdots H_2O]^{\bullet+}$ unpaired spin density at the B3LYP/DZP++ level.

Zero point vibrational energy (ZPVE) effects were applied to E_{HYD} to obtain hydration enthalpies at 0 K for all $[GC\cdots H_2O]^{\bullet+}$ equilibrium structures. For each species on the right-hand side of eq 2, the B3LYP/DZP++ harmonic ZPVEs were combined with ZAPT2/aug-cc-pVDZ electronic energies. The vibrational frequencies were also used to distinguish between minima and first-order saddle points.

The electronic charge distribution for each radical cation trimer was determined by natural bond orbital (NBO) partial charges[63−65] located on atomic centers. B3LYP/DZP++ electron densities were used in the analysis. The fraction of positive charge allocated to each monomer was found by totaling the NBO partial charge on its nuclei. The adiabatic ionization potentials (IP_{ad}) for guanine, the GC base pair, and GC monohydrate were calculated as $E_{G+} - E_G$, $E_{GC+} - E_{GC}$, and $E_{GC\text{-}H2O+} - E_{GC\text{-}H2O}$, respectively, at the B3LYP/DZP++ level of theory. IP_{ad} for the monohydrated base pair was calculated from the energies at the global minimum structures for the neutral and cation complexes.

Results and Discussion

The species formed from oxidation of guanine−cytosine monohydrate is a strongly interacting, noncovalently bound cluster of radical cation guanine, cytosine, and water. The *ab initio* and DFT methods employed in this work describe the ground state of the initial photoionization kinetic product. The calculated physical properties−spin density, charge distribution, electrostatic potential, hydration energy, and ionization potential−are associated with ground state stable intermediates formed prior to low-barrier chemical processes, which ultimately engenders "direct-type"[1] DNA damage.

Spin Density. In the oxidized state of the monohydrated guanine−cytosine nucleic acid base pair, only guanine exhibits significant radical character. Low-temperature ESR and ENDOR studies of various systems ranging in complexity from crystalline guanine to aqueous/glassy oligionucleotides or DNA report that the radical center is located on guanine.[66−73] A recent study shows that subsequent deprotonation of the guanine radical occurs in mid to high pH environments,[74] leaving the spin density largely undisturbed. The B3LYP/DZP++ spin density mapped over the spatial extent of the trimer (see Figure 2) indicates that the single unpaired electron is delocalized within the π system of guanine.

Electrostatic Potential. Electrostatic potentials (ESP) are useful for predicting intermolecular interaction strengths and sites.[75] The ESP of $[GC]^{\bullet+}$ is presented in Figure 3. The most striking feature of the electrostatic potential is that it does not mimic the spatial extent of the positive charge distribution. These ESP values are a measure of how strong the charge on $[GC]^{\bullet+}$ is felt by an approaching water molecule. The electrostatic contribution to the hydration energy arises primarily from a

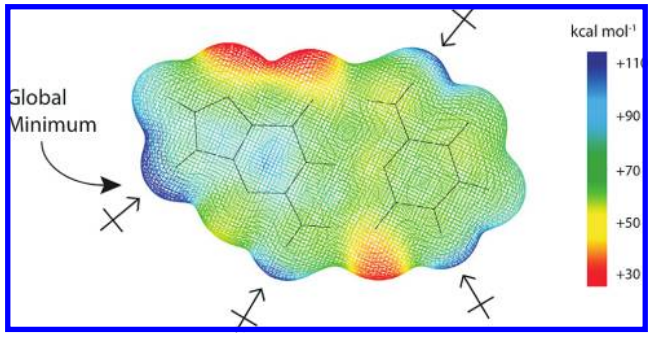

Figure 3. [GC]•+ electrostatic potential. Arrows indicate dipole orientations of interacting molecules. Blue denotes the most positive regions. Red indicates the least positive regions.

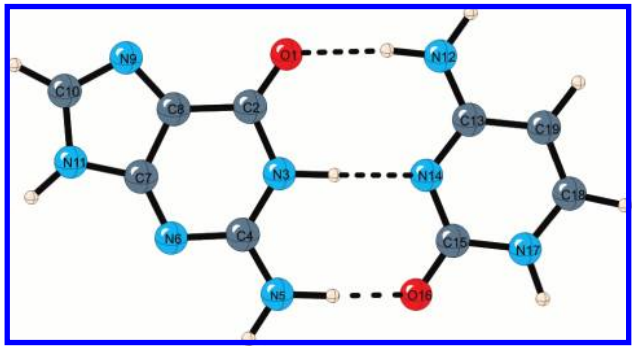

Figure 4. Qualitative structure of the guanine−cytosine radical cation.

charge−dipole interaction. According to the computed ESP, interaction sites near cytosine can yield comparable hydration energies to interaction sites near guanine despite the partial charge disparity between the two monomers. Electrostatic fields produced by ions have long-range effects that can direct and orient dipolar molecules that are not adjacent to the molecular ion.

Interaction Energy and Ionization Potential of [GC]•+. The structure of the guanine−cytosine radical cation is shown in Figure 4. The Watson−Crick interaction energy (ΔE_{WC}) of G•+−C evaluated with ZAPT2/aug-cc-pVDZ at B3LYP/DZP++ optimized geometries is 49.2 kcal mol^{-1}. Values obtained from previous studies range from 40.5 to 48.4 kcal mol^{-1}.[76−79] Zero-point vibrational effects decrease the interaction energy by 2.3 kcal mol^{-1}. This exceptionally strong molecular interaction arises from a network of ionic hydrogen bonds between the nucleic acid bases and a favorable alignment of large molecular dipoles of G•+ and C.[27,80]

Strongly interacting molecules can cause large distortions in the electronic structure of the monomers. Dramatic shifts in the electron density due to polarization or charge transfer lead to significant changes in the ionization potential. At the B3LYP/DZP++ level of theory, the adiabatic IP of isolated guanine is 7.63 eV. Formation of the Watson−Crick base pair lowers the calculated (B3LYP/DZP++) IP_{ad} of guanine to 6.88 eV. Hydrogen bonds formed upon hydration will drop the ionization potential lower. The ionization potential of the monohydrated base pair is 6.71 eV. Much experimental and theoretical effort has been dedicated to the determination of ionization potentials of nucleic acid bases within DNA in an aqueous environment.[81−87]

Structures and Hydration Energies. Eleven stationary points were located on the [GC···H_2O]•+ potential energy surface (PES). Hydration sites are defined as regions near [GC]•+ at which a minimum or transition state exists. Three

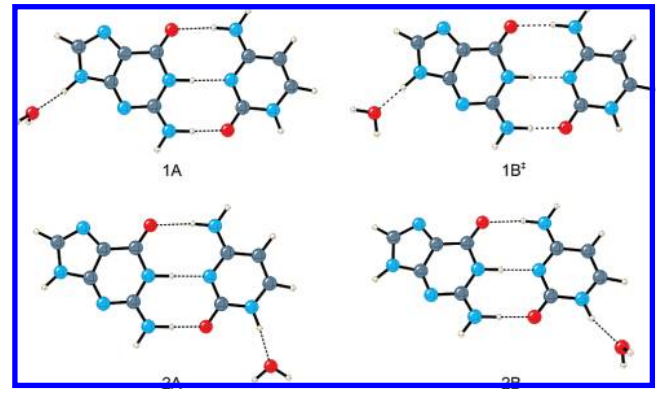

Figure 5. Four structures illustrating water interacting at the glycosidic bond sites of the guanine−cytosine radical cation.

TABLE 1: [GC]•+ Hydration Energies in kcal mol^{-1}

	ΔE_{HYD} B3LYP	ΔE_{HYD} SCF	ΔE_{HYD} correlation	ΔE_{HYD} ZAPT2	ΔH_{HYD} ZAPT2(B3LYP)
glycosidic					
1A	13.3	11.2	3.0	14.2	12.6
1B‡	12.9	10.8	2.9	13.7	12.3
2A	10.6	7.7	3.9	11.6	10.3
2B	10.4	7.3	4.0	11.4	10.3
groove					
3	10.2	7.7	3.6	11.3	9.6
4A	10.1	7.8	3.3	11.1	9.7
4B‡	10.0	7.7	3.3	11.0	9.7
5	6.7	5.1	3.4	8.5	7.3
face					
6	6.6	7.0	2.4	9.4	8.2
wedged					
7‡	8.1	7.7	0.8	8.5	7.3
8‡	6.8	5.5	1.6	7.1	6.2

hydration sites (1, 2, and 4) accommodate two distinct equilibrium structures connected by rotation about the water dipolar axis. At two different hydration sites (7 and 8) only transition states are present, while the remaining three hydration sites (3, 5, and 6) are each responsible for a single minimum on the trimer surface. The equilibrium structures are categorized according to the type of interaction it would make with double-helix DNA if the entire macro-molecule were present. Structures with water interacting near N_{11} and N_{17} are termed "glycosidic" (**1A**, **1B‡**, **2A**, **2B**). Structures for which the water is near N_{12} and N_{16} (**3**, **4A**, **4B‡**, **5**) are termed "groove" as these water molecules would exist in either the major or minor DNA groove. In "wedged" structures (**7‡** and **8‡**) water molecules interacting near C_{10} and C_{18} would be cornered in the sugar−phosphate backbone. Finally, a "face" structure (**6**) refers to the interaction of water above the plane of guanine. At all reported stationary points, water is oriented such that the negative end of its dipole is directed toward the base pair.

At the global minimum, **1A**, water is interacting at the glycosidic site of guanine (Figure 5). Water is perpendicular to the plane of [GC]•+ such that one hydrogen atom is above and one is below. The ΔE_{HYD} of **1A** is 2.6 kcal mol^{-1} larger than ΔE_{HYD} at any secondary minima. Table 1 gives the hydration energies for all equilibrium structures. The structure with the second largest ΔE_{HYD}, **1B‡**, is a transition state, and the imaginary mode is associated with water rotation out of the plane along water's dipolar axis. The rotational barrier at hydration site 1 is 0.5 kcal mol^{-1}. Water interacts most strongly with [GC]•+ at hydration site 1 due to the large partial positive charge on H−N_{11} and proximity to the cation.

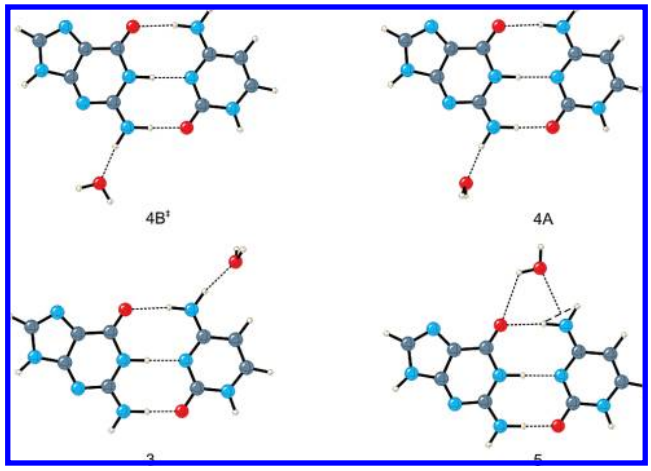

Figure 6. Structures of $[GC\cdots_2O]\bullet^+$ in which water is located in the major or minor groove of double-helix DNA.

TABLE 2: Hydrogen-Bond Distances (Å) Measured from Heavy Atom Positions[a]

	Gua−$O_1\cdots$ N_{12}−Cyt	Gua−$N_3\cdots$ N_{14}−Cyt	Gua−$N_5\cdots$ O_{16}−Cyt	H_2− $O\cdots$
glycosidic				
1A	2.944 (−0.013)	2.833 (0.007)	2.681 (0.018)	2.787
1B	2.944 (−0.013)	2.834 (0.008)	2.679 (0.016)	2.800
2A	2.951 (−0.006)	2.812 (−0.014)	2.638 (−0.025)	2.836
1B	2.955 (−0.002)	2.813 (−0.013)	2.634 (−0.029)	2.849
groove				
3	2.989 **(0.032)**	2.817 (−0.009)	2.614 **(−0.049)**	2.942
4A	2.938 **(−0.019)**	2.840 (0.014)	2.707 **(0.044)**	2.857
4B‡	2.937 **(−0.020)**	2.839 (0.013)	2.705 **(0.042)**	2.851
5	2.978 **(0.021)**	2.820 (−0.006)	2.639 **(−0.024)**	2.878
face				
6	2.949 (−0.008)	2.834 (0.008)	2.680 (0.017)	2.978
wedged				
7‡	2.947 (−0.010)	2.832 (0.006)	2.676 (0.013)	3.145
8‡	2.958 (0.001)	2.817 (−0.009)	2.647 (−0.016)	3.252

[a] Numbers in parentheses are differences between $[GC\cdots H_2O]\bullet^+$ and $[GC]\bullet^+$ values. Figures 5−8 describe the different structures.

Unlike the other hydration sites, two minima occur at glycosidic site 2, **2A** and **2B**. ΔE_{HYD} at these minima differ by 0.2 kcal mol^{-1}. Although water is positioned near cytosine in **2A** and **2B**, ΔE_{HYD} is reduced by only ∼20% compared to **1A** and **1B**‡. The direct interaction of water with G^+ remains significant throughout regions of the $[GC\cdots_2O]\bullet^+$PES in which water and guanine are not adjacent.

The interaction of water in a groove structure (Figure 6) incites changes in the hydrogen-bond network between guanine and cytosine. Absolute hydrogen-bond distances and differences between distances compared to the unhydrated base pair are given in Table 2. The largest change occurs at hydration site 3, where the water neighbors the amino group on cytosine. Electron density from water disrupts the local dipole on the amino group, weakening the Gua−$N_5\cdots O_{16}$−Cyt hydrogen bond. Subsequently, guanine and cytosine rock away from each other, opening one side and drawing the other side of the set of hydrogen-bonds closed. Similar effects occur for each groove structure.

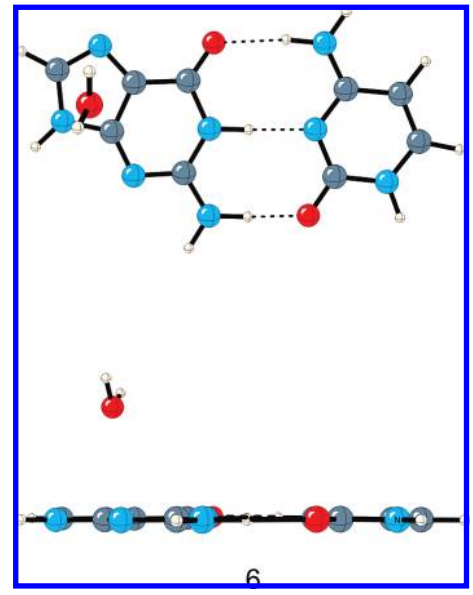

Figure 7. A structure in which water interacts above the plane of guanine in $[GC\cdots H_2O]\bullet^+$. Top and side views.

Three of the four groove structures have hydration energies comparable to **2A** and **2B**. The exception, **5**, has a ΔE_{HYD} that is at least 2.5 kcal mol^{-1} less than each of the glycosidic and groove structures and has an inherently different interaction between the water and base. In **5** a cyclic/cooperative hydrogen bond is formed between $O_1\cdots HO\cdots 2HN_{12}$. The oxygen atom on water forms a bifurcated hydrogen bond with the cytosine amino group. Two stationary points, a minimum and a transition state, occur at hydration site 4. The rotational barrier of water around its dipolar axis at site 4 is a tiny 0.1 kcal mol^{-1}.

The interaction of water above the plane of guanine (Figure 7) gives rise to the minimum **6** with a binding energy of 9.4 kcal mol^{-1}. Face minima have not been reported for hydration of neutral nucleic acid base pairs.[41] In this work, a minimum on the $[GC\cdots H_2O]\bullet^+$ surface was not found corresponding to water above the plane of cytosine. The correlation energy for structure **6** is a modest 25% of the total hydration energy, which suggests that the attraction is primarily electrostatic, with peripheral dispersion effects. Here, the charge−dipole interaction continues to be the dominant interaction, even without the formation of a typical ionic hydrogen bond upon hydration.

The two wedged structures shown in Figure 8 are both transition states and have the highest energy of any class of hydration structures. ΔE_{HYD} of **8**‡ is half that of the global minimum, **1A**. The imaginary mode is associated with rotation of water about its dipolar axis. Unlike hydration sites 1, 2, and 4, minima do not occur with the water perpendicular to the base pair. The CH···O interaction is weaker than NH···O interactions, allowing for water molecules to rotate and drift to nearby glycosidic sites, resulting in an overall stabilization of the complex. However, the sugar−phosphate backbone would stabilize **7**‡ and **8**‡ in their respective nucleotide structures.

Structures of ionic clusters obtained with the B3LYP functional[76,88] have proven reliable and adequate for the purposes of this work. Hydration energies computed with the B3LYP/DZP++ method are a notable improvement over SCF/aug-cc-pVDZ hydration energies with the one exception of the face

TABLE 3: Positive Charge Distributions in $[GC\cdots H_2O]^{\bullet+}$[a]

	guanine	cytosine	water
glycosidic			
1A	81.6	14.0	4.4
1B‡	81.6	14.0	4.4
2A	82.9	13.6	3.5
2B	82.9	14.0	3.1
groove			
3	83.2	14.4	2.5
4A	83.6	13.2	3.2
4B‡	83.4	13.3	3.3
5	82.9	16.6	0.5
face			
6	85.2	14.1	0.7
wedged			
7‡	84.1	14.3	1.6
8‡	83.7	15.3	1.0

[a] Values are percentages of total charge. Structures **1**−**8** are displayed in Figures 5−8.

structure (Table 1). The SCF value of 7.0 kcal mol^{-1} is closer to the ZAPT2 value of 9.4 kcal mol^{-1} than 6.6 kcal mol^{-1} obtained with B3LYP. For all structures besides **5** and **6**, B3LYP consistently underestimates ΔE_{HYD} at the ZAPT/aug-cc-pVDZ level by approximately 1 kcal mol^{-1}.

Charge Distribution. The protonation state of crystalline DNA-like systems can be determined through ENDOR spectra.[66] Oxidized guanine acts as a sufficient acid and can deprotonate under certain conditions.[74] Our density functional calculations on $[GC\cdots H_2O]^{\bullet+}$ reveal that barrierless deprotonation does not occur at 0 K in the gas phase upon oxidation. The acidic nature of oxidized guanine is observed through an increase in the proton donor bond lengths of 0.027 and 0.035 Å for N_3-H and N_5-H, respectively. Furthermore, NBO partial charges were evaluated in order to determine the redistribution of charge to the noncovalently bound water and cytosine molecules. Hydration and formation of the Watson−Crick pair cause small changes in the electron distribution, amounting to a 15−20% net loss of positive charge on guanine. The majority of this positive charge is acquired by cytosine, and the amount gained by water varies for different structures. The percentage of charge localized on each monomer for all $[GC\cdots H_2O]^{\bullet+}$ structures is given in Table 3.

The greatest redistribution of the electron density occurs for the lowest energy structures. At the glycosidic hydration sites, the partial positive charge on water is larger than at the groove, face, or wedged sites. Formation of the base pair produces a more significant change in the electron density than the change resulting from hydration. The degree of positive charge localized on cytosine is larger than the charge gained by water by a factor of 3. In fact, the ratio of partial charges, δ^+_{water} to δ^+_{cyt}, resembles the ratio of interaction energies, E_{HYD} to E_{WC}. The capacity for charge migration within $[GC\cdots H_2O]^{\bullet+}$ makes an important contribution to the hydration of $[GC]^{\bullet+}$ and is a feature for which static field theories provide reasonable results.

The mismatching of radical centers and positive charge can be attributed to the fact that the interaction of water with the σ-type electronic orbitals does not disrupt the π-electron distribution. For that reason, the face structure presents an atypical situation in which positive charge gained by water is minimal, but the electron hole density may extend over the interacting oxygen atom. Long-range hole migration through the base stack is governed by overlapping π-type orbitals.[89−94] It appears that radical sites move through DNA parallel to the base stack, and charge migrates in a more perpendicular fashion.

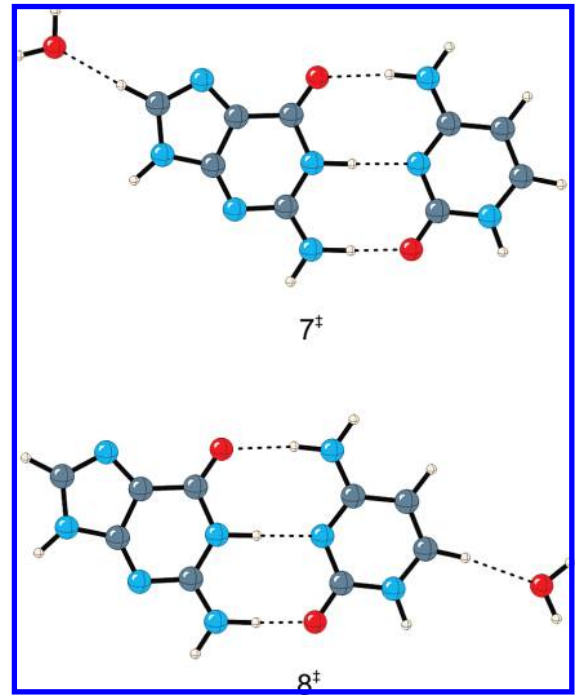

Figure 8. Structures of $[GC\cdots H_2O]^{\bullet+}$ where the water molecule is wedged near the sugar phosphate backbone.

Electron holes have been shown to migrate through the DNA base stack over moderate distances.[15] One of the factors contributing to the trapping ability of guanine is the fast deprotonation to the hydrogen-bonded cytosine moiety. The subsequent separation of charge and spin inhibits radical reactivity.

Conclusions

The fate of an irradiated molecule is highly dependent on its immediate environment. Formation of hydrogen bonds contributes to the increased hole activity on the nucleic acid bases.[16,17,37,95] Electron densities are redistributed upon the formation of hydrogen bonds, leading to the delocalization of positive charge. This redistribution of positive charge over noncovalently bound molecules acts to lower the ionization potential of guanine and other nucleic acid bases. We have shown that hydration at the glycosidic bond sites is responsible for the largest shift of electron density toward $G^{\bullet+}$ and the largest hydration energy of 14.2 kcal mol^{-1}.

Water plays an integral role in direct radiation processes of DNA. Initially, water participates in the photoionization of DNA by absorbing radiation and transferring the hole directly to the backbone or the peripheral edge of nucleic acid bases. A more subtle effect of hydration is softening the ionization potential for nucleic acid bases, which facilitates long-range charge migration to the guanine sink. Monohydration can also cause changes in the Watson−Crick hydrogen-bond distances. A water molecule that binds in the double-helix groove disrupts and weakens the hydrogen-bond network. The importance of water in radiation biology extends far beyond the scope of primary direct radiation products. But, by incorporating water into radiation targets in computational investigations, the mechanisms of DNA damage and repair may become better understood.

Acknowledgment. This work was supported by the U.S. National Science Foundation, Grant CHE-0749868. Select calculations were run at Pittsburgh Supercomputing Center under Teragrid Project CHE-070038N, Grant CHE-070010P. Figures

1−5 were generated using HFSmol.[96] We thank Dr. Steven Wheeler for many helpful discussions.

Supporting Information Available: Equilibrium geometries (B3LYP/DZP++) for all $[GC\cdots H_2O]^{\bullet+}$ trimers, GC (neutral and cation), guanine cation, cytosine, and water; absolute energies at the B3LYP/DZP++ and ZAPT2/aug-cc-pVDZ levels; zero-point vibrational energies. This material is available free of charge via the Internet at http://pubs.acs.org.

References and Notes

(1) Becker, D.; Sevilla, M. D. Chemical Consequences of Radiation Damage to DNA. In *Advances in Radiation Biology*; Lett, J. T., Sinclair, W. K., Eds.; Academic Press, Inc.: San Diego, 1993; Vol. 17, pp 121−180.

(2) Cadet, J.; Douki, T.; Gasparutto, D.; Ravanat, J. L. *Radiat. Phys. Chem.* **2005**, *72*, 293–299.

(3) Cadet, J.; Douki, T.; Ravanat, J. L. *Acc. Chem. Res.* **2008**, *41*, 1075–1083.

(4) Cullis, P. M.; Davis, A. S.; Malone, M. E.; Podmore, I. D.; Symons, M. C. R. *J. Chem. Soc., Perkin Trans. 2* **1992**, 1409–1412.

(5) Gräslund, A.; Ehrenberg, A.; Rupprecht, A.; Ström, G. *Biochim. Biophys. Acta* **1971**, *254*, 172–186.

(6) Gregoli, S.; Olast, M.; Bertinchamps, A. *Radiat. Res.* **1982**, *89* (2), 238–254.

(7) Hüttermann, J.; Voit, K.; Oloff, H.; Köhnlein, W.; Gräslund, A.; Rupprecht, A. *Faraday Discuss. Chem. Soc.* **1984**, *78*, 135–149.

(8) Krisch, R. E.; Flick, M. B.; Trumbore, C. N. *Radiat. Res.* **1991**, 126.

(9) Marguet, S.; Markovitsi, D.; Talbot, F. *J. Phys. Chem. B* **2006**, *110* (23), 11037–11039.

(10) Nelson, W. H.; Sagstuen, E.; Hole, E. O.; Close, D. M. *Radiat. Res.* **1992**, *131* (1), 10–17.

(11) Purkayastha, S.; Bernhard, W. A. *J. Phys. Chem. B* **2004**, *108* (47), 18377–18382.

(12) Purkayastha, S.; Milligan, J. R.; Bernhard, W. A. *J. Phys. Chem. B* **2006**, *110* (51), 26286–26291.

(13) Symons, M. C. R. *Radiat. Phys. Chem.* **1995**, *45*, 837–845.

(14) Hüttermann, J. *Ultramicroscopy* **1982**, *10*, 25–40.

(15) Cai, Z. L.; Sevilla, M. D. , Studies of excess electron and hole transfer in DNA at low temperatures. In *Long-Range Charge Transfer in DNA II*; Schuster, G. B., Ed.; Springer: Berlin, 2004; pp 103−127.

(16) Debije, M. G.; Strickler, M. D.; Bernhard, W. A. *Radiat. Res.* **2000**, *154* (2), 163–170.

(17) Purkayastha, S.; Milligan, J. R.; Bernhard, W. A. *Radiat. Res.* **2006**, *166* (1), 1–8.

(18) Bernhard, W. A. *J. Phys. Chem.* **1989**, *93* (6), 2187–2189.

(19) Gregoli, S.; Olast, M.; Bertinchamps, A. *Radiat. Res.* **1979**, 77.

(20) Sevilla, M. D.; Becker, D.; Yan, M.; Summerfield, S. R. *J. Phys. Chem.* **1991**, *95* (8), 3409–3415.

(21) Sevilla, M. D.; D'Arcy, J. B.; Morehouse, K. M.; Engelhardt, M. L. *Photochem. Photobiol.* **1978**, 29.

(22) Symons, M. C. R. *J. Chem. Soc., Faraday Trans. 1* **1987**, *83*, 1–11.

(23) Close, D. M. *Radiat. Res.* **1997**, *147* (6), 663–673.

(24) Hole, E. O.; Nelson, W. H.; Sagstuen, E.; Close, D. M. *Radiat. Res.* **1992**, *129* (2), 119–138.

(25) Cauet, E.; Dehareng, D.; Lievin, J. *J. Phys. Chem. A* **2006**, *110* (29), 9200–9211.

(26) Colson, A. O.; Besler, B.; Close, D. M.; Sevilla, M. D. *J. Phys. Chem.* **1992**, *96* (2), 661–668.

(27) Elshakre, M. *Int. J. Quantum Chem.* **2005**, *104*, 1–15.

(28) Hush, N. S.; Cheung, A. S. *Chem. Phys. Lett.* **1975**, *34* (1), 11–13.

(29) Nir, E.; Grace, L.; Brauer, B.; de Vries, M. S. *J. Am. Chem. Soc.* **1999**, *121* (20), 4896–4897.

(30) Orlov, V. M.; Smirnov, A. N.; Varshavsky, Y. M. *Tetrahedron Lett.* **1976**, (48), 4377–4378.

(31) Russo, N.; Toscano, M.; Grand, A. *J. Comput. Chem.* **2000**, *21*, 1243–1250.

(32) Verkin, B. I.; Sukhodub, L. F.; Yanson, I. K. *Dokl. Akad. Nauk Sssr* **1976**, *228* (6), 1452–1455.

(33) Barnett, R. N.; Cleveland, C. L.; Landman, U.; Boone, E.; Kanvah, S.; Schuster, G. B. *J. Phys. Chem. A* **2003**, *107* (18), 3525–3537.

(34) Belau, L.; Wilson, K. R.; Leone, S. R.; Ahmed, M. *J. Phys. Chem. A* **2007**, *111* (31), 7562–7568.

(35) Colson, A. O.; Besler, B.; Sevilla, M. D. *J. Phys. Chem.* **1993**, *97* (51), 13852–13859.

(36) Zhu, Q.; LeBreton, P. R. *J. Am. Chem. Soc.* **2000**, *122* (51), 12824–12834.

(37) O'Neill, P.; Fielden, E. M. Free Radical Processes in DNA. In *Advances in Radiation Biology*; Lett, J. T., Sinclair, W. K., Eds.; Academic Press, Inc.: San Diego, 1993; Vol. 17, pp 53−120.

(38) Danilov, V. I.; Tolokh, I. S. *J. Mol. Struct.:THEOCHEM* **1985**, *123* (1−2), 109–119.

(39) Kabelac, M.; Hobza, P. *Phys. Chem. Chem. Phys.* **2007**, *9* (8), 903–917.

(40) Pohorile, A.; Burt, S. K.; MacElroy, R. D. *J. Am. Chem. Soc.* **1984**, *106*, 402–409.

(41) Zendlova, L.; Hobza, P.; Kabelac, M. *ChemPhysChem* **2006**, *7* (2), 439–447.

(42) Abo-Riziq, A.; Crews, B.; Grace, L.; de Vries, M. S. *J. Am. Chem. Soc.* **2005**, *127* (8), 2374–2375.

(43) Crews, B.; Abo-Riziq, A.; Grace, L.; Callahan, M.; Kabeláč, M.; Hobza, P.; de Vries, M. S. *Phys. Chem. Chem. Phys.* **2005**, *7*, 3015–3020.

(44) Danilov, V. I.; Mourik, T. v.; Poltev, V. I. *Chem. Phys. Lett.* **2006**, *429*, 255–260.

(45) Gadre, S. R.; Babu, K.; Rendell, A. P. *J. Phys. Chem. A* **2000**, *104* (39), 8976–8982.

(46) Kim, N. J.; Kim, Y. S.; Jeong, G.; Ahn, T. K.; Kim, S. K. *Int. J. Mass Spectrom.* **2002**, *219* (1), 11–21.

(47) Kim, S.; Wheeler, S. E.; Schaefer, H. F. *J. Chem. Phys.* **2006**, *124* (20), 204310–8.

(48) Piuzzi, F.; Mons, M.; Dimicoli, I.; Tardivel, B.; Zhao, Q. *Chem. Phys.* **2001**, *270* (1), 205–214.

(49) Pullman, B.; Miertus, S.; Perahia, D. *Theor. Chim. Acta* **1979**, *50* (4), 317–325.

(50) Saigusa, H.; Mizuno, N.; Asami, H.; Takahashi, K.; Tachikawa, M. *Bull. Chem. Soc. Jpn.* **2008**, *81* (10), 1274–1281.

(51) Sukhanov, O. S.; Shishkin, O. V.; Gorb, L.; Leszczynski, J. *Struct. Chem.* **2008**, *19* (1), 171–180.

(52) Yamaguchi, T.; Nagata, C. *J. Theor. Biol.* **1977**, *69* (4), 693–707.

(53) Close, D. M.; Crespo-Hernández, C. E.; Gorb, L.; Leszczynski, J. *J. Phys. Chem. A* **2008**, *112*, 4405–4409.

(54) Liu, D.; Wyttenbach, T.; Bowers, M. T. *J. Am. Chem. Soc.* **2006**, *128* (47), 15155–15163.

(55) Shao, Y.; Fusti-Molnar, L., Jung, Y.; Kussmann, J.; Ochsenfeld, C.; Brown, S. T.; Gilbert, A. T. B.; Slipchenko, L. V.; Levchenko, S. V.; O'Neill, D. P.; Distasio, R. A., Jr.; Lochan, R. C.; Wang, T.; Beran, G. J. O.; Besley, N. A.; Herbert, J. M.; Lin, C. Y.; Voorhis, T. V.; Chien, S. H.; Sodt, A.; Steele, R. P.; Rassolov, V. A.; Maslen, P. E.; Korambath, P. P.; Adamson, R. D.; Austin, B.; Baker, J.; Byrd, E. F. C.; Dachsel, H.; Doerksen, R. J.; Dreuw, A.; Dunietz, B. D.; Dutoi, A. D.; Furlani, T. R.; Gwaltney, S. R.; Heyden, A.; Hirata, S.; Hsu, C.-P.; Kedziora, G.; Khalliulin, R. Z.; Klunzinger, P.; Lee, A. M.; Lee, M. S.; Liang, W.; Lotan, I.; Nair, N.; Peters, B.; Proynov, E. I.; Pieniazek, P. A.; Rhee, Y. M.; Ritchie, J.; Rosta, E.; Sherrill, C. D.; Simmonett, A. C.; Subotnik, J. E.; Woodcock, H. L. III.; Zhang, W.; Bell, A. T.; Chakraborty, A. K.; Chipman, D. M.; Keil, F. J.; Warshel, A.; Hehre, W. J.; Schaefer, H. F.; Kong, J.; Krylov, A. I.; Gill, P. M. W.; Head-Gordon, M. *Phys. Chem. Chem. Phys.* **2006**, *8*, 3172−3191.

(56) Dunning, T. H., Jr. *J. Chem. Phys.* **1970**, 53.

(57) Huzinaga, S. *J. Chem. Phys.* **1965**, 42.

(58) Lee, T. J.; Schaefer, H. F. *J. Chem. Phys.* **1985**, 83.

(59) Dunning, T. H., Jr. *J. Chem. Phys.* **1989**, 90.

(60) Kendall, R. A.; Dunning, T. H., Jr.; Harrison, R. J. *J. Chem. Phys.* **1992**, 96.

(61) Kawahara, S.; Uchimaru, T. *Phys. Chem. Chem. Phys.* **2000**, *2*, 2869–2872.

(62) Riley, K. E.; Hobza, P. *J. Phys. Chem. A* **2007**, *111* (33), 8257–8263.

(63) Foster, J. P.; Weinhold, F. *J. Am. Chem. Soc.* **1980**, *102*, 7211–7218.

(64) Reed, A. E.; Weinhold, F. *J. Chem. Phys.* **1983**, *78*, 4066–4073.

(65) Reed, A. E.; Weinstock, R. B.; Weinhold, F. *J. Chem. Phys.* **1985**, *83*, 735–746.

(66) Close, D. M. *Radiat. Res.* **1993**, *135* (1), 1–15.

(67) Close, D. M.; Nelson, W. H.; Sagstuen, E.; Hole, E. O. *Free Radical Res. Commun.* **1989**, *6* (2−3), 83–85.

(68) Close, D. M.; Sagstuen, E.; Nelson, W. H. *J. Chem. Phys.* **1985**, *82* (9), 4386–4388.

(69) Hole, E. O.; Nelson, W. H.; Close, D. M.; Sagstuen, E. *J. Chem. Phys.* **1987**, *86* (9), 5218–5219.

(70) Hole, E. O.; Sagstuen, E.; Nelson, W. H.; Close, D. M. *Free Radical Res. Commun.* **1989**, *6* (2−3), 87–90.

(71) Jayatilaka, N.; Nelson, W. H. *J. Phys. Chem. B* **2007**, *111* (27), 7887–7896.

(72) Jayatilaka, N.; Nelson, W. H. *J. Phys. Chem. B* **2007**, *111* (4), 800–810.

(73) Sagstuen, E.; Hole, E. O.; Nelson, W. H.; Close, D. M. *Free Radical Res. Commun.* **1989**, *6* (2−3), 91–92.

(74) Adhikary, A.; Kumar, A.; Becker, D.; Sevilla, M. D. *J. Phys. Chem. B* **2006**, *110* (47), 24171–24180.

(75) Murray, J. S.; Politzer, P. In *Quantum Medicinal Chemistry*; Carloni, P.; Alber, F. Ed.; Wiley-VCH: Weinheim, Germany, 2003.
(76) Bertran, J.; Oliva, A.; Rodriguez-Santiago, L.; Sodupe, M. *J. Am. Chem. Soc.* **1998**, *120* (32), 8159–8167.
(77) Han, S. Y.; Lee, S. H.; Chung, J.; Oh, H. B. *J. Chem. Phys.* **2007**, *127* (24), 245102–10.
(78) LiX. F.; SevillaM. D. DFT treatment of radiation produced radicals in DNA model systems. *Advanced Quantum Chemistry*; Academic Press, Inc.: San Diego, CA, 2007; Vol. 52, pp 59−87.
(79) Reynisson, J.; Steenken, S. *Phys. Chem. Chem. Phys.* **2002**, *4*, 5346–5352.
(80) Hobza, P.; Šponer, J. *Chem. Rev* **1999**, 99.
(81) Close, D. M.; Crespo-Hernandez, C. E.; Gorb, L.; Leszczynski, J. *J. Phys. Chem. A* **2005**, *109* (41), 9279–9283.
(82) Crespo-Hernandez, C. E.; Arce, R.; Ishikawa, Y.; Gorb, L.; Leszczynski, J.; Close, D. M. *J. Phys. Chem. A* **2004**, *108* (30), 6373–6377.
(83) Hutter, M. C. *Chem. Phys.* **2006**, *326* (1), 240–245.
(84) Kim, N. S.; Zhu, Q.; LeBreton, P. R. *J. Am. Chem. Soc.* **1999**, *121* (49), 11516–11530.
(85) Kim, S. K.; Lee, W.; Herschbach, D. R. *J. Phys. Chem.* **1996**, *100* (19), 7933–7937.
(86) Li, X.; Cai, Z.; Sevilla, M. D. *J. Phys. Chem. B* **2001**, *105* (41), 10115–10123.
(87) Steenken, S.; Jovanovic, S. V. *J. Am. Chem. Soc.* **1997**, *119* (3), 617–618.
(88) Tureček, F. Computational studies of radicals relevant to nucleic acid damage. *Advanced Quantum Chemistry*; Academic Press, Inc.: San Diego, CA, 2007;*Vol 52*, 89−120.
(89) Becker, D.; Vere, T. L.; Sevilla, M. D. γ-Irradiation of the hydration layer of DNA: μOH formation vs hole transfer. In *Radiation Damage in DNA Structure/Function Relationships at Early Times*; Fuciarelli, A. F., Zimbrick, J. D., Eds.; Battelle Press: Columbus, OH, 1995.
(90) Giese, B. *Acc. Chem. Res.* **2000**, *33* (9), 631–636.
(91) Joy, A.; Schuster, G. B. *Chem. Commun.* **2005**, (22), 2778–2784.
(92) Sartor, V.; Boone, E.; Schuster, G. B. *J. Phys. Chem. B* **2001**, *105* (45), 11057–11059.
(93) Schuster, G. B.; Landman, U. The mechanism of long-distance radical cation transport in duplex DNA: Ion-gated hopping of polaron-like distortions. In *Long-Range Charge Transfer in DNA I*; Springer-Verlag: Berlin, 2004; Vol. 236, pp 139−161.
(94) Senthilkumar, K.; Grozema, F. C.; Guerra, C. F.; Bickelhaupt, F. M.; Lewis, F. D.; Berlin, Y. A.; Ratner, M. A.; Siebbeles, L. D. A. *J. Am. Chem. Soc.* **2005**, *127* (42), 14894–14903.
(95) Douki, D.; Ravanat, J. L.; Angelov, D.; Wagner, J. R.; Cadet, J. Effects of duplex stability on charge-transfer efficiency within DNA. In *Long-Range Charge Transfer in DNA I*; Springer-Verlag: Berlin, 2004; Vol. 236, pp 1−25.
(96) Wheeler, S. E. *HFSmol*; University of Georgia, Athens, GA, 2008.

JP900444K